

## Hyperbolic Secant RF Pulses for Simultaneous Multi-Slice Excitation with Reduced Susceptibility Artifacts

Mehran Baboli<sup>1</sup>, Bastien Guerin<sup>2</sup>, Lawrence Wald<sup>2</sup>, and V. Andrew Stenger<sup>1</sup>

<sup>1</sup>Medicine, University of Hawaii, Honolulu, Hawaii, United States, <sup>2</sup>Radiology, Massachusetts General Hospital, Massachusetts, United States

**Target Audience:** Physicists, engineers, and neuroscientists interested in RF pulse design for simultaneous multi-slice imaging.

**Purpose:** To demonstrate Multiband (MB) and Power Independent of Number of Slices (PINS) Hyperbolic Secant (HS) RF pulses for simultaneous multi-slice (SMS) excitation with reduced through-plane signal loss for gradient echo applications such as fMRI.

**Introduction:** HS RF pulses can be used to generate a quadratic phase in the slice-select direction to reduce susceptibility induced signal dropout in regions including the frontal lobe of brain and are useful for applications such as fMRI [1-3]. Recently SMS imaging techniques have been shown to provide speed increases by factors up to 12 in fMRI applications [4, 5]. Typically SMS excitation is accomplished by using a modulated sinc MB RF pulse. Additionally the PINS pulse design has been proposed for low power SMS excitation using a series of non-selective pulses separated by z-gradient blips [6, 7]. This study demonstrates both MB and PINS SMS excitations weighted by an HS envelope to reduce susceptibility artifacts in the brain at 3T.

**Methods:** MB RF pulses  $B_{MB}(t)$  obtain SMS excitation of  $N$  slices separated by  $\Delta z$  by summing modulated pulses with pulse profile  $p(t)$ :

$$B_{MB}(t) = p(t) \sum_{n=1}^N e^{i\gamma G_z t \Delta z n}.$$

Typically a sinc function is used for  $p(t)$ . The PINS pulse  $B_{PINS}(t)$  is constructed as a train of rectangular sub-pulses weighted by  $p(t)$ :

$$B_{PINS}(t) = p(t) \text{rect}(t/T) \sum_{l=0}^L \delta(t - lT).$$

Where  $L$  is the number of sub-pulses and z-gradient blips of duration  $T$ . To generate a quadratic phase in the slice profile,  $p(t)$  is set as an HS pulse defined by amplitude  $A(t)$  and phase  $\phi(t)$  [3]:

$$A(t) = A_0 \text{sech}(\beta t) \text{ and } \phi(t) = \mu \ln[\text{sech}(\beta t)] + \mu \ln A_0$$

Where  $A_0$  is the maximum amplitude,  $\beta$  is the modulation frequency, and  $\mu$  is a dimensionless parameter to control sharpness of the slice profile and the degree of quadratic phase. To remove excess ripple in the slice profile, a Gaussian filter was applied to the RF pulse. Figs. 1 and 2 show examples of HS-MB and HS-PINS SMS pulses with  $\mu=3$ ,  $\beta=1824\text{Hz}$ , and  $N=8$ . Also shown are the slice profiles for the pulses matched for the same slice profile with 3mm thickness. Images of the human brain were acquired in a normal adult volunteer using a Siemens TIM Trio VB17 3T scanner with a 32-channel head coil. Eight slices were acquired using (A) a standard sinc MB pulse, (B) an HS-MB pulse, (C) a standard PINS pulse, and (D) an HS-PINS pulse to observe the effect on recovering signal loss. A fully sampled 3D FLASH sequence was used for SMS imaging with parameters of FOV=20cm, slice thickness=3mm, gap=10mm, TE=25ms and TR=50ms.

**Results and Discussion:** Fig. 3 shows the images acquired with the four SMS pulses. Column (A) shows the eight slices simultaneously acquired by the standard sinc MB pulse. Columns (B) and (C) and (D) show the same slices when HS-MB, standard PINS and HS-PINS pulses respectively. Comparing the four sets of images shows the partial signal recovery with HS-MB and HS-PINS pulses, as a result of canceling the susceptibility gradient by the quadratic phase. Regions of signal recovery are shown with yellow arrows. Although there was reduced signal dropout, there was a small overall decrease in SNR due to increased signal loss in the rest of the brain. Future studies will examine the use of the pulse for SMS fMRI applications.

**Acknowledgements:** This work was supported R01DA019912, R01EB011517, and K02DA02056.

**References:** [1] Cho *et al.* MRM 23, 193 (1992); [2] Shmueli *et al.* ISMRM 14, 2385 (2006); [3] Wastling *et al.* (2014); [4] Feinberg *et al.* PlosOne 5, 1 (2010); [5] Setsompop *et al.* MRM 67, 1210 (2012); [6] Norris *et al.* MRM 66, 1234 (2011); [7] Anderson *et al.* MRM 72, 1342 (2004).

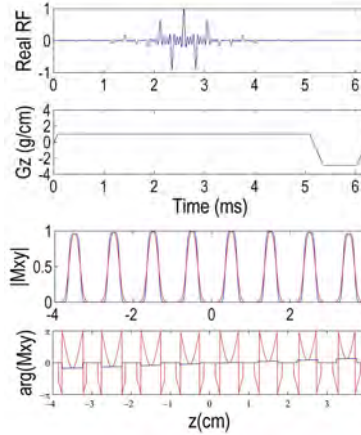


**Fig. 1** HS-MB RF pulse and its slice profile (red) in comparison with a standard sinc MB pulse (blue).

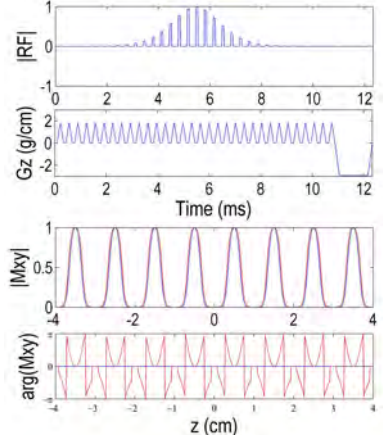


**Fig. 2** HS-PINS RF pulse and its slice profile (red) in comparison with a standard PINS pulse (blue).

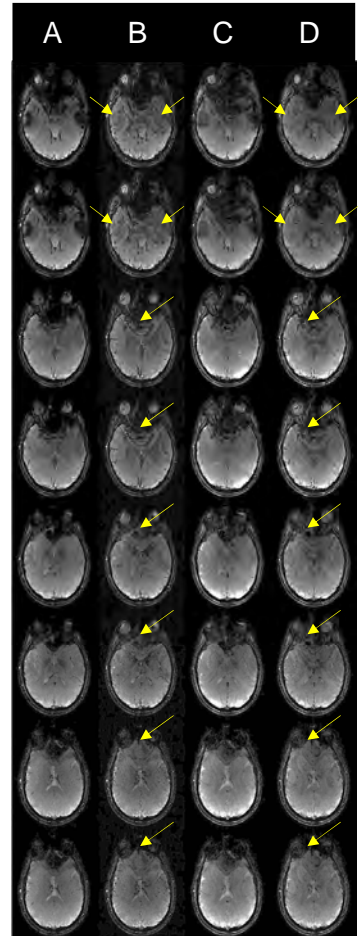


**Fig. 3** Human brain images acquired at 3T using (A) standard sinc MB (B) HS-MB (C) standard PINS and (D) HS-PINS pulses.